

Effect of relaxation of the second-nearest neighbors on the thermodynamic properties of semiconducting alloys: Application to $\text{GaAs}_y\text{Sb}_{1-y}$

A. Qteish

*Dipartimento di Fisica, Università di Roma II, Via E. Carnevale, 00173 Roma, Italy
and Consiglio Nazionale delle Ricerche, Istituto di Acustica, Via Cassia 1216, 00189 Roma, Italy*

N. Motta and A. Balzarotti

*Dipartimento di Fisica, Università di Roma II, Via E. Carnevale, 00173 Roma, Italy
(Received 16 June 1988)*

We have studied the effect of relaxation of the second-nearest neighbors (NNN's) in $\text{GaAs}_y\text{Sb}_{1-y}$ alloys by introducing a simple model which takes into account the difference in volume among the various configurations of the basic cluster. Using state-of-the-art density-functional theory, the ground-state properties of five different ordered structures have been calculated. It has been found that none of them is thermodynamically stable. Fixing the NNN overestimates by about 50% the strain energy and gives a miscibility gap of the disordered alloy larger than experiment, while upon relaxing the NNN excellent agreement with experiment is obtained.

I. INTRODUCTION

In spite of the technological importance of semiconducting alloys the present understanding of their thermodynamic properties is far from satisfactory.^{1,2} The experimental determination of the phase diagram of these materials is a difficult problem, and it has been done only for a very limited number of alloys. Recently, some theoretical calculations have been performed using a combined electronic structure and statistical-mechanical approach.^{3,4} In these calculations the tetrahedron (four-site and five-site tetrahedron for ternary³ and binary⁴ alloys, respectively) is considered as the basic building unit; only one of the fcc sublattices is allowed to relax (the unmixed sublattice in the case of ternary alloys) to allow for the bond length alternation. The second-nearest-neighbor (NNN) relaxation in the mixed sublattice is thus completely neglected. This relaxation should not be confused with the equilibrium volume relaxation introduced by Zunger and co-workers,⁵ since in the latter the various configurations are assumed to have the same volume. Even so, the effects of the two relaxations are more or less the same, but the involved approximations are very different.

Previously, only phenomenological approaches were undertaken. Balzarotti and co-workers⁶ have studied the thermodynamic properties of some ternary semiconducting alloys using elastic energies calculated by the valence-force-field (VFF) method⁷ and chemical energies extracted from the experimental values of the interaction parameter. This approach gives a positive chemical contribution to the formation energies of the ordered structures, contrary to the present understanding. More refined calculations on the same line have been carried out by Patrick, Chen, and Sher,⁸ where more structural relaxation (up to the third shell) is allowed and the chemical contribution is calculated using Harrison's bonding

theory.⁹ However, the most recent first-principles work of Mbaye, Ferreira, and Zunger³ has shown that proper accounting for the chemical energy is essential and leads to new features in the phase diagram.

Very recently the present authors have introduced¹⁰ a new scheme for calculating the thermodynamic properties of semiconducting alloys from the total energy of five ordered structures, which correspond to the different tetrahedral configurations. This scheme is very similar to the one described above, but here the lattice parameter $a(y)$ is assumed to be different for the various cluster configurations. Previously, the cluster energies at fixed composition were assumed to be equal to the formation energy of the ordered structures having the same lattice parameter $a(y)$ of the alloy. The new scheme takes into account the fact that in the disordered alloy the different cluster configurations have different volumes, and thus allows for the NNN relaxation. It should be noticed that the vertices of the tetrahedra are still assumed to occupy the ideal zinc-blende lattice sites. This is very important since the cluster energies can be calculated self-consistently without any additional effort.

Unlike other semiconducting alloys, several experimental investigations of the solid-solid phase diagram of $\text{GaAs}_y\text{Sb}_{1-y}$ have been carried out. It has been found that this system has a large miscibility gap, $0.2 < y < 0.8$ at 1018 K,¹¹⁻¹³ and around this temperature the solid-solid and solid-liquid phase diagrams overlap. Recently, ordered structures (AuCu-I and chalcopyrite type) have been observed in $\text{GaAs}_{0.5}\text{Sb}_{0.5}$ alloy superlattice grown on InP substrate¹⁴ (i.e., well inside the miscibility gap). Ordered structures in other semiconducting alloy superlattices¹⁵⁻²⁰ have been also observed. The present understanding is that these ordered structures are metastable, and the ordering is just a moderate tendency toward complete segregation.

This work is devoted to study the effect of NNN relax-

ation on the GaAs_ySb_{1-y} alloys. The total energy as a function of the structural parameters for the different ordered structures has been calculated using state-of-the-art density-functional theory.²¹ It has been found that none of these structures is thermodynamically stable, which shows that the recently observed ordered structures¹⁴ are metastable. The phase diagram of this material has been constructed using the energies calculated above with relaxed and unrelaxed NNN distances. Both the modified quasicheical approximation (QCA) of Guggenheim²² and the cluster variation method (CVM) of Kikuchi^{23,24} have been used to calculate the configurational entropy. It has been found that neglecting the NNN relaxation overestimates by a factor of 2 the strain (positive) energy and leads to a larger miscibility gap than experimentally observed. Instead, the relaxed model gives excellent agreement with experiment. This shows that the latter scheme is much more realistic than the previous one, and that earlier results^{3,4} obtained with fixed NNN distances should be taken with caution.

The present work is organized as follows. In Sec. II we describe in detail the method to calculate the thermodynamic properties of semiconducting alloys. In Sec. III we give the computational details and results obtained for the five different ordered structures. Section IV is devoted to Monte Carlo calculations and results. In Sec. V we report and discuss our results for the thermodynamic properties of disordered GaAs_ySb_{1-y} alloys. Section VI contains a discussion of the accuracy of the proposed model. Finally, in Sec. VII we draw our main conclusions.

II. METHOD

A. Basic assumptions

The calculation of the thermodynamic properties of alloys is a formidable problem since it requires the knowledge of the partition function, defined as a sum over the probability of all possible states of the system. However, the calculation of these properties can be done by introducing the following simplifying assumptions.²³

(1) The summation in the partition function is replaced by the most probable state which has the minimum free energy. Thus the problem is reduced to find this state out of a very large and unavailable set of states.

(2) Instead of dealing with the whole system, we consider small clusters of sites (subsystems) known as basic clusters. Of course, the accuracy will increase by increasing the size of these clusters.

(3) The basic clusters in the alloy are energetically independent and the energy of each configuration can be realized by coherently ordered structures containing only this configuration. This is exactly the assumption which allows for the use of the first-principles self-consistent (SC) calculations.

According to the second assumption, the Helmholtz or, equivalently in this case, the Gibbs free energy of mixing can be written as

$$G = \Delta E(y, T) - TS(y, T), \quad (1)$$

where S is the configurational entropy, and ΔE is the enthalpy of mixing given as

$$\Delta E = \sum_{i,j,k,l} z_{ijkl} \Delta E_{ijkl}. \quad (2)$$

Here the four-site tetrahedron is considered as the basic cluster and summation is over all its possible configurations. z_{ijkl} and ΔE_{ijkl} are the concentration and the formation energy of the $ijkl$ th cluster, respectively. The configurational entropy S is also a function of the basic cluster concentration z . Therefore, the equilibrium Gibbs free energy of mixing, $G_{\text{eq}}(y, T)$, the entropy, and the variables z are determined by minimizing G with respect to the independent variables z at a fixed point in the (y, T) plane. The equilibrium lattice parameter $a_{\text{eq}}(y, T)$ can be calculated by minimizing G_{eq} with respect to a .

Up to now, in all SC calculations of the formation energy of the cluster configuration, the tetrahedron is taken as a basic cluster. For pseudobinary semiconducting alloys, such as AB_3C_{1-y} , where only one of the sublattices is alloyed, a four-site tetrahedron similar to that of the fcc lattice can be considered. This is not the case for binary semiconducting alloys.⁴ For the four-site tetrahedron there are 2^4 configurations. However, not all of them are different, but only five, A_n , where $n = 0, 1, 2, 3, 4$ is the number of B atoms at the vertices.

B. Cluster energies

The formation energy of each configuration, A_n , is determined from a SC total-energy calculation performed for the ordered structure having this particular configuration. The prototype ordered structures which contain few atoms per unit cell (up to eight) are shown in the inset of Fig. 5. It is worth mentioning that in this calculation only the inside atom is allowed to relax, in order to accommodate the difference in length of the alloyed bonds, while the mixed sublattice is kept fixed. Using symmetry arguments, the distortion of the inside atom is thus determined by a single scalar parameter δ , defined as d/d_0 , where d is the length of the bond along the relaxation direction in the case of the cubic structure, and the Ga-Sb interplanar distance in the case of the tetragonal structure. The formation energies of the periodic structures—which are considered as those of the corresponding tetrahedral configurations—as a function of the structural parameters are

$$\Delta E_{A_n} = \Delta E_{A_n}(a, \delta) - \left[\frac{n}{4} E_{AB} + \frac{(4-n)}{4} E_{AC} \right], \quad n = 0, \dots, 4 \quad (3)$$

where E_{AB} and E_{AC} are the energies of the pure materials at their equilibrium volumes. The cluster energies of the disordered alloys, $\Delta E_{ijkl}(y)$, are the key quantities in the thermodynamic calculations. In the following we will describe and discuss two models to determine $\Delta E_{ijkl}(y)$ from the formation energies calculated for the ordered structures.

1. Model A

EXAFS measurements have shown that the NNN relaxation of the *alloyed atoms*, the anions in the present case, is small compared to the first nearest-neighbor (NN) relaxation. For example, in the case of²⁵ $\text{Ga}_y\text{In}_{1-y}\text{As}$ the relaxation parameter for the AB bond, defined as $\epsilon_{AB} = (R_{AB} - R_{AC}^0)/(R_{AB}^0 - R_{AC}^0)$ and similarly for the AC bond, is equal to 0.85 for the InAs bond near the GaAs end, and 0.76 for the GaAs bond near the InAs end. In the case of a similarly defined relaxation parameter for the In-In and Ga-Ga NNN distances, the estimated values are 0.18 and 0.29, respectively. For this reason the NNN relaxation is completely neglected in the previous calculations^{3,4} (i.e., the different tetrahedral configurations are assumed to have equal volumes). In this case the cluster energy as a function of y can be given as

$$\Delta E_n(y) = E_n(a(y), \delta_{\text{eq}}) - \left[\frac{n}{4} E_{AB} + \frac{(4-n)}{4} E_{AC} \right], \quad n=0, \dots, 4 \quad (4)$$

where $a(y)$ is the lattice parameter of the alloy which follows closely Vegard's law; δ_{eq} is the equilibrium relaxation parameter of the n th configuration calculated at $a(y)$.

Since the different clusters are assumed to have the same volume, which is in fact not the case in real alloys, this model overestimates the strain energy and gives a miscibility gap larger than the experimentally determined one, as it will be shown later.

2. Model B

The main artifact of model A is that NNN distances between the alloyed atoms are kept fixed. In the model we propose here, this assumption is relaxed simply by assigning different values of $a(y)$ to the different configurations at fixed y . So Eq. (4) is rewritten as

$$\Delta E_n(y) = E_n(a_n(y), \delta_{\text{eq}}) - \left[\frac{n}{4} E_{AB} + \frac{(4-n)}{4} E_{AC} \right], \quad n=0, \dots, 4. \quad (5)$$

The variation with y of the lattice parameter of the tetrahedral configurations, $a_n(y)$, is assumed to be linear. All $a_n(y)$ are assumed to be parallel and equally spaced; $a_0(0)$ and $a_4(1)$ are equal to those of the corresponding pure materials. The interspacing distance can be determined from the constraint (see Sec. IV) that the calculated average NNN distances coincide with the experimental values, if possible, or with the distances calculated from a much more relaxed calculation using, for instance, the valence-force-field model.²⁵

The advantage of this model is that it allows for the NNN relaxation using state-of-the-art density-functional theory without any additional effort. The proposed method avoids lengthy and costly calculations on large supercells to include NNN relaxation. Note carefully that even in the latter case, the relaxation is structure

dependent (i.e., does not simulate the random alloy). As will be shown later, in this model the relaxation energy is reduced by a factor of 2 and the calculated phase diagram is in excellent agreement with experiment.

C. Configurational entropy

Taking into consideration our basic clusters, an approximate entropy can be calculated using QCA or CVM. In QCA the basic clusters are assumed to be statistically independent and the entropy is given as⁶

$$S^{\text{QCA}} = -k_B \left[\sum_i y_i \ln y_i + \sum_{i,j,k,l} (z_{ijkl}^{(B)}) \ln z_{ijkl}^{(B)} - z_{ijkl} \ln z_{ijkl} \right], \quad (6)$$

where y_i is the concentration of atom i (B or C). The superscript B refers to the Bernoulli distribution (completely random distribution of the B and C atoms in the alloyed sublattice). In CVM, the entropy for the four-site tetrahedron is given as²³

$$S^{\text{CVM}} = -k_B \left[5 \sum_i y_i \ln y_i - 6 \sum_{i,j} y_{ij}^{(2)} \ln y_{ij}^{(2)} + 2 \sum_{i,j,k,l} z_{ijkl} \ln z_{ijkl} \right], \quad (7)$$

where $y^{(2)}$ denotes the concentration of the NNN pairs. The appearance of the concentration of the subclusters in the S^{CVM} expression, which are the overlap regions between the basic clusters and the subclusters of nonvanishing contribution, introduces some statistical correlation between clusters in the alloy. Therefore S^{CVM} is commonly believed to be more accurate than QCA; however, for disordered alloys at high temperature, both approximations give the same results.

Once the cluster energies are calculated and an entropy expression is adopted, the Gibbs free energy of mixing, G , can be minimized with respect to the independent variables z to calculate G_{eq} , z , and S , from which other thermodynamic functions can be easily determined.

D. Basic equations and definitions

In the last two subsections the framework for calculating the cluster energy and the configurational energy was presented. Here we describe in more detail how the calculation of the thermodynamic properties is performed. As discussed above, the independent cluster variables z_{ijkl} and the entropy can be determined by minimizing G with respect to z_{ijkl} . This should be done under the constraint⁶

$$\sum_{i,j,k,l} (n_{ijkl} - 4y) z_{ijkl} = 0, \quad (8)$$

where n_{ijkl} is the number of B atoms in the $ijkl$ th cluster, which takes into account both the fixed concentration and the normalization condition (the sum of the variable z is equal to 1). Therefore the free energy to be minimized is

$$G(y, T) = \sum_{i,j,k,l} z_{ijkl}(y, T) \Delta E_{ijkl} - TS(y, T) + \lambda \sum_{i,j,k,l} (n_{ijkl} - 4y) z_{ijkl}(y, T), \quad (9)$$

where the formation energies ΔE_{ijkl} are calculated according to Eqs. (4) or (5) and λ is the Lagrange parameter. In the case of QCA, the minimization of G with respect to z_{ijkl} is straightforward and gives

$$z_{ijkl}(y, T) = \frac{\xi^{(n_{ijkl}-4y)} e^{-\Delta E_{ijkl}/k_B T}}{\sum_{i,j,k,l} \xi^{(n_{ijkl}-4y)} e^{-\Delta E_{ijkl}/k_B T}}, \quad (10)$$

where $\xi = e^{-\lambda/k_B T}$ is a positive and real quantity, which can be determined by solving the fourth-order polynomial equation

$$\sum_{i,j,k,l} (n_{ijkl} - 4y) \xi^{(n_{ijkl}-4y)} e^{-\Delta E_{ijkl}/k_B T} = 0. \quad (11)$$

For the case of CVM, minimizing G with respect to the independent variables z_{ijkl} gives

$$z_{ijkl}(y, T) = \frac{Y^{-5/8} Y_2^{1/2} \xi^{(n_{ijkl}-4y)/2} e^{-\Delta E_{ijkl}/2k_B T}}{\sum_{i,j,k,l} Y^{-5/8} Y_2^{1/2} \xi^{(n_{ijkl}-4y)/2} e^{-\Delta E_{ijkl}/2k_B T}}, \quad (12)$$

where

$$Y = y_i y_j y_k y_l$$

and

$$Y_2 = y_{ij}^{(2)} y_{ik}^{(2)} y_{il}^{(2)} y_{jk}^{(2)} y_{jl}^{(2)} y_{kl}^{(2)}.$$

The subcluster variables y and $y^{(2)}$ are dependent variables which can be written in terms of independent variables z . The system of nonlinear equations, Eq. (12), can be solved self-consistently using the natural interaction method of Kikuchi,²⁶ starting with guess values for the dependent variables and solving a fourth-order polynomial similar to Eq. (11) during every iteration. Having calculated the tetrahedral concentration z , the thermodynamic functions can be calculated easily. The entropy and the Gibbs free energy are given as in Eqs. (6) or (7) and Eq. (1), respectively.

From the equilibrium Gibbs free energy G_{eq} , the phase

diagram (miscibility gap and spinodal curve) can be easily calculated. The instability region in the (y, T) space, bounded by the spinodal curve, is the region where

$$\frac{\partial^2 G_{eq}(y, T)}{\partial y^2} < 0, \quad (13)$$

while the miscibility gap, above which disordered alloys are stable, can be calculated from the values of y at which $G_{eq}(y)$ have common tangent at fixed T .

The excess Gibbs free energy of mixing is given as²⁷

$$G^e(y, T) = G_{eq}(y, T) - k_B T [y \ln y + (1-y) \ln(1-y)], \quad (14)$$

the second term being the free energy of mixing of the ideal system. From $G^e(y, T)$ the interaction parameter Ω is calculated as

$$\Omega(y, T) = G^e(y, T) / y(1-y). \quad (15)$$

Finally, as a measure of the deviation from randomness (clustering) we follow Jones *et al.*²⁸ in defining the clustering parameter

$$\Delta(y, T) = y_{12}^{(2)} - y(1-y) = \sum_{i,j} z_{12ij} - y(1-y), \quad (16)$$

which is the excess mixed NNN pair probability distribution.

III. COMPUTATIONAL DETAILS AND RESULTS FOR THE ORDERED STRUCTURES

The prototypical structures which realize the different tetrahedral configurations are shown in the inset of Fig. 5. The total energy as a function of the structural parameters, a and δ , for the above structures is performed in the framework of density-functional theory (DFT),²¹ using the local-density approximation²⁹ (LDA) and norm-conserving pseudopotentials.³⁰ For the exchange and correlation we use the data of Ceperley and Alder,³¹ as parametrized by Perdew and Zunger.³² The pseudopotentials are taken from the tabulation of Bachelet *et al.*³³ The special- k -point technique of Baldereschi³⁴ is used to integrate over the Brillouin zone; the two Chadi-Cohen³⁵ special points are used for the zinc-blende structure, while an equivalent set of points³⁶ has been used for each of the other structures. The one-particle wave functions

TABLE I. Theoretical values of the equilibrium lattice parameter, bulk modulus, formation energy, relaxation parameter, and relaxation energy for the five considered ordered structures.

System	Lattice parameter (Å)	Bulk modulus (Mbar)	Formation energy (mRy/atom)	Relaxation parameter	Relaxation energy (mRy/atom)
GaSb	5.96	0.53			
Ga ₄ Sb ₃ As	5.86	0.58	1.41	0.963	-1.91
Ga ₂ SbAs	5.76	0.74	2.11	1.064	-1.93
Ga ₄ SbAs ₃	5.63	0.83	1.50	1.032	-1.40
GaAs	5.56	0.61			

are expanded in plane waves with a constant energy cutoff $E_{\text{cut}} = 12$ Ry. Such cutoff is found to give excellent results for the Si-Ge system.³⁷

The total energy of each of the above ordered structures as a function of a has been calculated as follows. The equilibrium relaxation parameter δ_{eq} and the relaxation energy ΔE^R have been calculated at some selected values of a . It has been found that δ_{eq} has a weak a dependence; for example, in the case of the tetragonal structure, corresponding to $y = 0.5$, the calculated δ_{eq} is 1.076 and 1.060 at $a = 10.4$ and $a = 11.4$ a.u., respectively, while ΔE^R is found to vary considerably with a . However, the difference between the equilibrium relaxation energies calculated with a fixed value of δ_{eq} —calculated at $a = ya_{\text{eq}}^{(\text{GaAs})} + (1-y)a_{\text{eq}}^{(\text{GaSb})}$ —and the exact ΔE_{min}^R is found to be very small, of the order of 10^{-5} Ry/atom. Therefore, to determine the ground state properties of the considered ordered structures, a fixed value of δ_{eq} is assumed; the total energy is then calculated as a function of the lattice constant at six points in steps of 0.2 a.u. around equilibrium and fitted to the Murnaghan's equation of state³⁸

$$E(V) = \frac{B_0 V}{B'_0} \left[\frac{(V_0/V)B'_0}{B'_0 - 1} + 1 \right], \quad (17)$$

where V_0 is the equilibrium volume, and B_0 and B'_0 are the bulk modulus and its pressure derivative at V_0 . The results of the fit are shown in Table I for the five ordered structures, each corresponding to a different composition y (multiple of 0.25): the variation of the lattice parameter is found to fulfill Vegard's law. The experimental values of B_0 are 0.56 and 0.75 Mbar for GaSb and GaAs, respectively. The small difference between theoretical and experimental values in the bulk moduli of GaAs and the unusual variation are artifacts of the rather small E_{cut} we are forced to use. It has been shown⁴ that this has negligible effects on the calculated thermodynamic properties.

The positive sign of the formation energies of the ordered structures reflects the instability of these structures toward segregation. Similar results have been obtained by Boguslawski and Baldereschi³⁹ for the tetragonal structure, where also the c/a relaxation is included. This leads us to the conclusion that the recently observed ordered structures in $\text{GaAs}_y\text{Sb}_{1-y}$ alloy superlattices are metastable. Our results confirm further that the reported ordered structures in semiconductor alloy superlattices^{37,39,40} are not thermodynamically stable, and the ordering is just a moderate tendency toward complete segregation.

A contour plot of the valence charge density of the unrelaxed tetragonal structure in the plane of the two bonds is shown in Fig. 1(a). In Fig. 1(b) we show a similar plot for pure GaAs (left panel) and GaSb (right panel) calculated at the same lattice parameter of the tetragonal structure. The important feature to notice is the large similarity between the bond charge density of Ga—As and Ga—Sb in the pure materials and the mixed structure, which demonstrates the transferability of the bond charge density. Similar results have been obtained for the Si-Ge system.³⁷ In Fig. 1(c) we show the non-zinc-blende

charge density $\Delta\rho$ of the tetragonal structure, which is the driving force of the structural relaxation,⁴¹ defined as

$$\Delta\rho = \rho_{AB}(r) - \frac{[\rho_A(r) + \rho_B(r)]}{2}, \quad (18)$$

where A (B) are GaAs (GaSb). The important features to

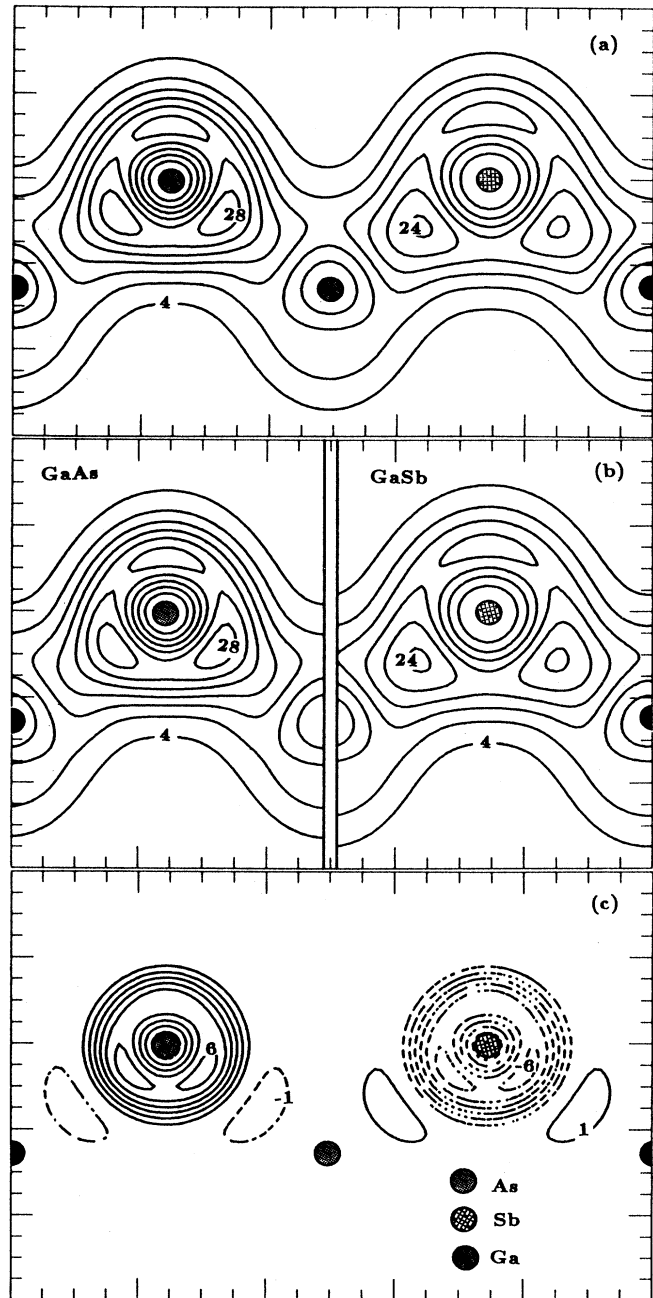


FIG. 1. Contour plot of the valence charge density (electron per zinc-blende unit cell) in the plane of the two bonds, in steps of 4, for (a) the unrelaxed tetragonal structure, (b) pure GaAs and GaSb. The non-zinc-blende charge density [Eq. (18)], in step of 1, is shown in (c). Dashed lines, negative; solid lines, positive.

note are the localization of $\Delta\rho$ around the As and Sb atoms and the large magnitude of $\Delta\rho$ compared with the result of Ref. 42. By relaxing the inside atom, a charge transfer from the less ionic Ga—Sb to the more ionic Ga—As bond occurs: before relaxation the maximum bond charge densities (in units of electron/zinc-blende-unit-cell) are 24.65 and 30.57 for Ga—Sb and Ga—As bond, respectively. After relaxation they are 23.65 and 31.35. Similar results are obtained by Srivastava *et al.*⁴²

The calculated Ga—As and Ga—Sb NN distances for GaAs and GaSb are shown by open circles in Fig. 2(a), and the average values ($\sqrt{3}a/4$) are shown by solid circles in the same figure. The relaxation of the above bond

is found to be smaller than experiment. This point is discussed in Sec. V.

IV. MONTE CARLO CALCULATIONS

The crucial assumption of model *A* is that the alloyed atoms are kept on the ideal zinc-blende sites and the five different basic structures have equal volume. This constraint raises the formation energy of the alloy to an extent which depends on the excess strain energy stored in each ordered unit. Any structural relaxation of the mixed sublattice will certainly lower this energy. The simplest way of doing this, while preserving the local symmetry, has been proposed in Sec. II B. To estimate the concentration dependence of the lattice parameter of the cluster configuration, a_n , we have generated the alloy lattice positions by means of a Monte Carlo simulation. The calculation was made using VFF. We write the elastic energy per tetrahedron as²⁵

$$E^{\text{el}} = \frac{3}{8r_0^2} \left[\sum_i \alpha_i [\Delta(\mathbf{r}_i \cdot \mathbf{r}_i)]^2 + \sum_s \sum_{i,j} \beta_{ij} [\Delta(\mathbf{r}_i^s \cdot \mathbf{r}_j^s)]^2 \right], \quad (19)$$

where α_i and β_{ij} are bond-stretching and bond-bending force constants,⁷ respectively, r_i is the bond length of the i th bond around the s base atom, and r^0 is the equilibrium bond length. We have carried out the alloy simulation for an arbitrary composition y by minimizing the elastic energy of randomly generated large clusters. In

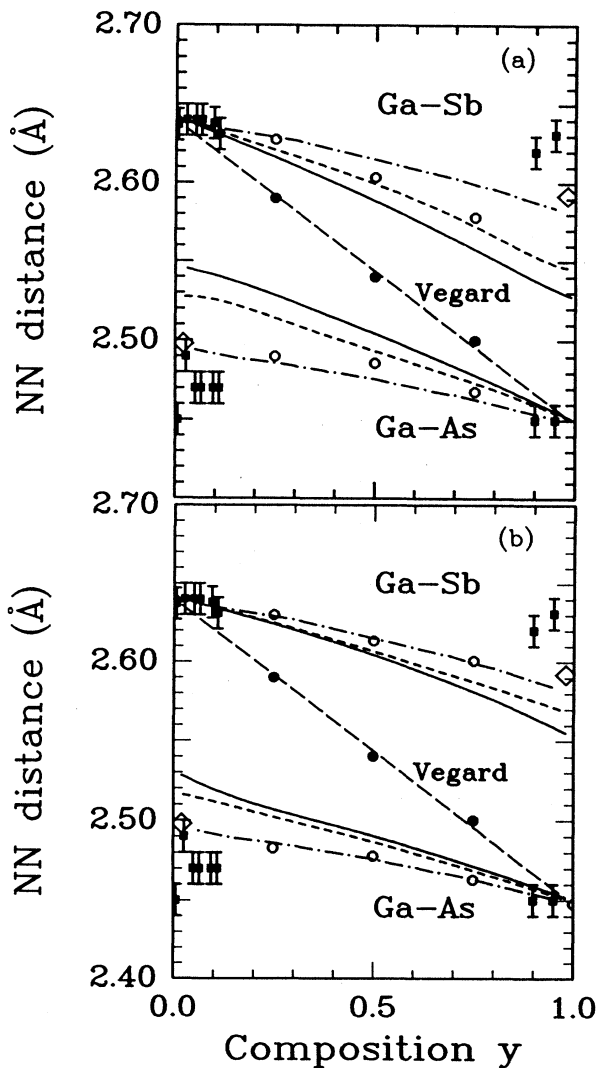


FIG. 2. First-nearest-neighbor (NN) distances as functions of composition y . (a) Self-consistent results. (b) Valence-force-field results. Open circles, ordered structures; solid circles, order structures averaged; solid lines, model *A* averaged; short-dashed lines, model *B* averaged. Compared with Vegard's law (long-dashed lines), Monte Carlo results (dashed-dotted lines), impurity model (diamonds), and EXAFS measurements (Ref. 47) (solid symbols).

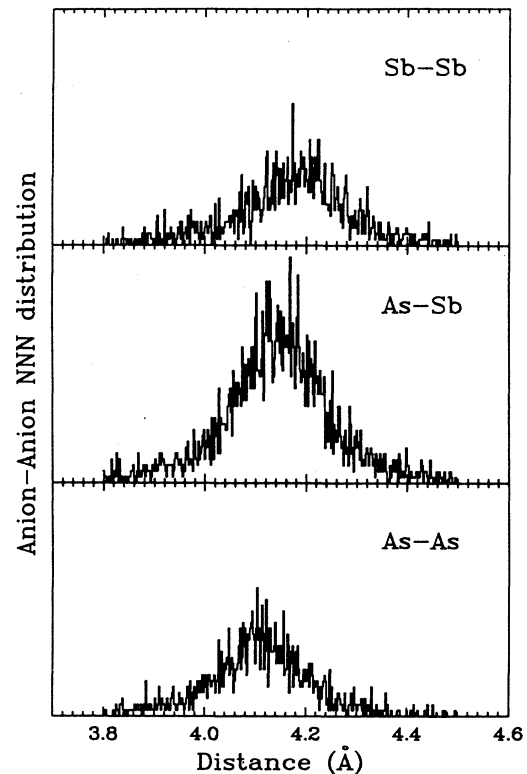


FIG. 3. Anion-anion NNN distances distributions for $\text{GaAs}_{0.5}\text{Sb}_{0.5}$ calculated by Monte Carlo.

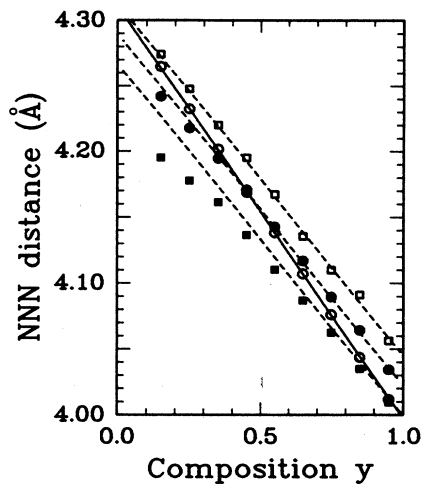


FIG. 4. Monte Carlo results for second-nearest-neighbor distances. Open squares, Sb-Sb; solid squares, As-As; solid circles, As-Sb; open circles, Monte Carlo average; solid line, Vegard's law; dashed lines, calculated average using model *B*.

order to nullify the cluster size effect, we have relaxed 7–8 shells of atoms around the central one. Averaging over 1000 configurations has been carried out in order to achieve good statistical convergence. The distribution of NNN distances for $y = 0.5$ are shown in Fig. 3.

To estimate the interspacing distance, required in model *B*, we have fitted the scaled calculated average NNN distances to those obtained by the Monte Carlo simulation. The interspacing distance which gives the best fit is found to be 0.06 a.u. In Fig. 4 we show the Monte Carlo results for NNN distances in the alloyed sublattice compared with the fitted results of model *B*. The fitting is good, showing a perfect matching of the two calculations. The deviation observed in the As-As distances at low As content is attributed to the stiffer and shorter Ga—As bond with respect to that of Sb. This effect, found in EXAFS experiments on impurities in a larger host matrix,⁴³ is known as “core size effect.” The approximations involved in the SC calculations do not produce such be-

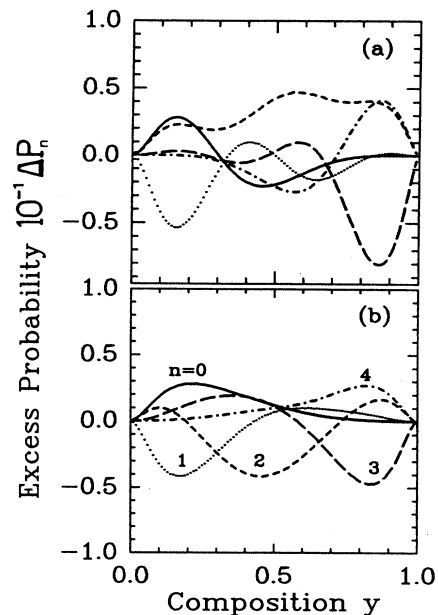


FIG. 6. Excess probability distributions of the tetrahedral configurations as functions of composition y . (a) Results of model *A*; (b) results of model *B*.

havior. Unfortunately, we can not compare our Monte Carlo results with EXAFS data because the latter are unavailable. For $\text{In}_{1-y}\text{Ga}_y\text{As}$ (Ref. 26) and $\text{Cd}_{1-y}\text{Zn}_y\text{Te}$ (Ref. 44) alloys, where this comparison is possible, they provide a good estimate of the structure of real alloys.

V. THERMODYNAMIC PROPERTIES OF DISORDERED $\text{GaAs}_y\text{Sb}_{1-y}$ ALLOYS

Using the formation energy of the ordered structures calculated in Sec. III, the cluster energies of mixing $\Delta E_n(y)$ as a function of the composition y , calculated according to the model *A* (solid lines) and the model *B* (dashed lines), are shown in Fig. 5 for the five different tetrahedral configurations. The remarkable feature to notice is the large reduction (about 50%) of the strain en-

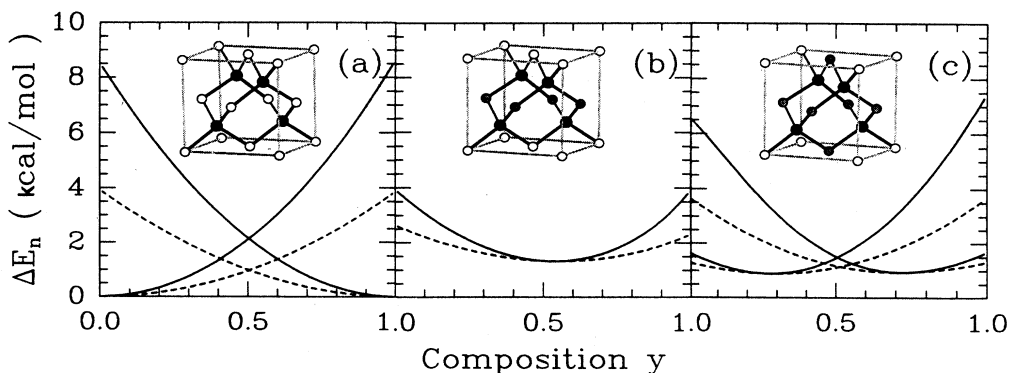


FIG. 5. Cluster formation energy as a function of composition y . Solid lines, model *A*; dashed lines, model *B*. For (a) Ga_0 and Ga_4 ; (b) Ga_2 ; (c) Ga_1 and Ga_3 , where n is the number of Sb atoms at the vertices. The corresponding ordered structures are also shown.

ergy calculated according to model *B*. Starting from the above calculated $\Delta E_n(y)$, the tetrahedral concentrations are calculated using Eq. (10) after solving Eq. (11) for the case of the QCA, and solving Eq. (12) self-consistently starting from random (Bernoulli) distribution of the dependent variables y and $y^{(2)}$. In Fig. 6(a) we show the results of model *A* for the excess probability distribution $\Delta P_n(y)$ [where P_n are the tetrahedral concentrations z times the degeneracy factor $\binom{4}{n}$] at $T=700$ K. In Fig. 6(b) similar results obtained using model *B* are shown. The important feature to notice is that the NNN relaxation not only affects the magnitude of ΔP_n but also the sign in some composition range, which is configuration dependent. This can be understood as a consequence of the large reduction of the strain energy in model *B*.

The calculated phase diagrams are shown in Fig. 7(a) using model *A* and in Fig. 7(b) using model *B*, compared with the experimentally determined miscibility gap. It is evident that the miscibility gap calculated using model *A* at $T=1020$ K is in the range $0.06 < y < 0.93$, while experimentally it is within the range $0.2 < y < 0.8$.¹¹⁻¹³ This is expected since the strain energy is overestimated within this model. On the other hand, the agreement between the experimental and calculated miscibility gap using model *B* is excellent. The small asymmetry of the

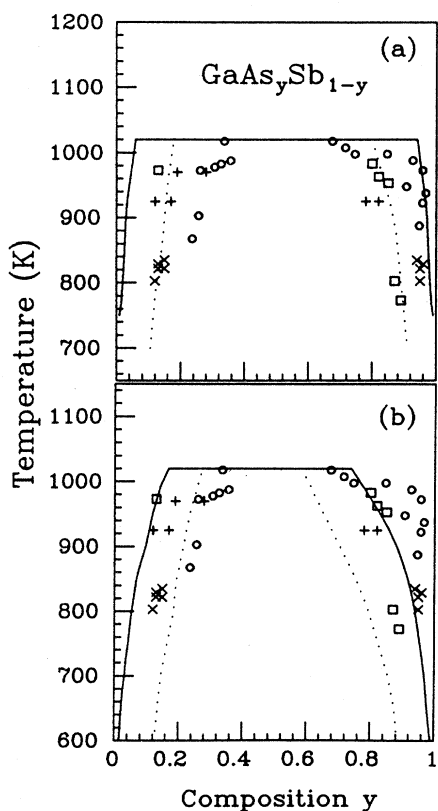


FIG. 7. Calculated phase diagram of $\text{GaAs}_y\text{Sb}_{1-y}$ alloys, using (a) model *A* and (b) model *B*. Solid lines, miscibility gap; dotted lines, spinodal curve. The experimental results for the miscibility gap of Refs. 12 (plus), 11 (open circle), 13 (cross), and 45 (open square) are also shown.

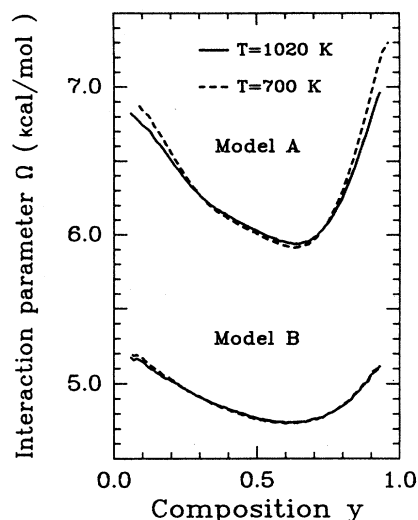


FIG. 8. Interaction parameter Ω as a function of composition y , calculated using model *A* (upper curves) and model *B* (lower curves). Solid lines, $T=1020$ K; dashed lines, $T=700$ K.

theoretical phase diagram should not be considered as an artifact of the calculation, since the experimental results of Pessetto and Stringfellow¹² and of Takenada *et al.*⁴⁵ do not show an asymmetric phase diagram as those of Gratton *et al.*¹¹ and Mani *et al.*¹³ However, the most remarkable feature here is the large effect of the NNN relaxation on the phase diagram of these materials which has been underestimated in previous theoretical calculations.^{3,4} The above results demonstrate the astonishing high predictive power of our approach. The importance of this result comes from the fact that the experimental determination of the phase diagram of the semiconducting alloys is difficult, and experimental results exist only for a few selected alloys.

In Fig. 8 we show the interaction parameter Ω calculated as a function of y at $T=700$ and $T=1020$ K, using the above two models. The remarkable features are the large difference between Ω calculated within the two models and the small temperature dependence. The latter is expected since the excess probability distribution ΔP_n is small (see Fig. 6) and it has small T dependence. In the case of model *B*, at $x=0.5$, Ω is equal to 4.75 kcal/mole compared with the experimentally estimated values 4.0, 4.27, and 4.5 kcal/mole,⁴⁶ which is another indication of the superiority of model *B* over model *A*.

The calculated average GaAs and GaSb NN distances using the SC relaxation parameter and the probability distribution at $T=1020$ K are shown in Fig. 2(a) using model *A* and model *B*, compared with the Vegard's law variation, the Monte Carlo results, the experimental results,⁴⁷ and the results of the impurity model.⁴⁸ The important features to notice are the following.

(i) All the theoretical approaches are unable to explain the observed large relaxation of the NN distances. In contrast, the Monte Carlo calculation or even the impurity model is able to provide excellent agreement with ex-

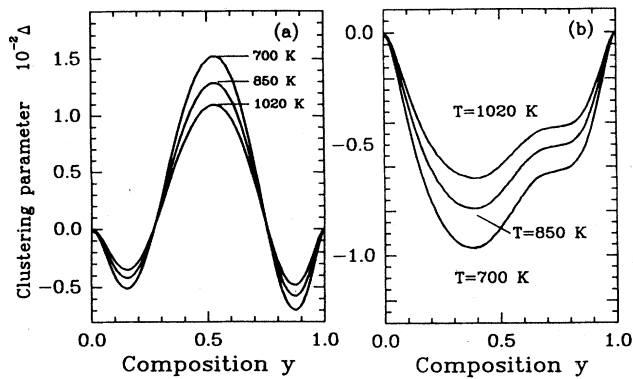


FIG. 9. Clustering parameter Δ as a function of composition y at different temperatures, calculated using (a) model A and (b) model B .

periment for many other ternary systems, such as $\text{Ga}_{1-y}\text{In}_y\text{As}$ (Ref. 25) and $\text{Cd}_{1-y}\text{Zn}_y\text{Te}$.⁴⁴ We remark, however, that EXAFS data taken in the transmission mode on dilute systems could be affected by considerable errors, particularly in the case of powdered samples, such as those measured here, which have a limited homogeneity.⁴⁹

(ii) The average NN distances, calculated using model B , are the same as those for the ordered structures. In fact the deviation found in model A is an artifact of the model (see Sec. VI). For sake of comparison, we show in Fig. 2(b) similar results obtained using VFF to determine the relaxation in the ordered structures. Notice the agreement between the Monte Carlo results and the bond lengths of the ordered structures.

It should be noticed that the calculated NN distances are very sensitive to the equilibrium relaxation parameter δ_{eq} which is calculated at a fixed volume. As already mentioned, the related change in energy is very small to affect our calculated thermodynamic properties.

In Fig. 9 we show the calculated clustering parameter [Eq. (16)] as a function of the composition y for various temperatures, calculated using model A [Fig. 9(a)] and model B [Fig. 9(b)]. It is clear that the effect of the NNN relaxation is also significant in this case.

VI. DISCUSSION

To discuss the accuracy of the calculated phase diagram using the two models described previously, we show in Fig. 10(a) the enthalpy of mixing calculated using the VFF model (both bond stretching and bond bending included), starting from ordered structures—exactly as in the first-principles calculations—within model A (solid line) and model B (dashed line). The result of the Monte Carlo, which simulates the real alloy, based on the same model and force constants (see Sec. IV) is also shown (dashed-dotted line). It is evident that the result of model B is much closer to the Monte Carlo result than that of model A . This shows the power of model B , and demonstrate the validity of the results obtained using this model. For comparison we show in Fig. 10(b) similar results

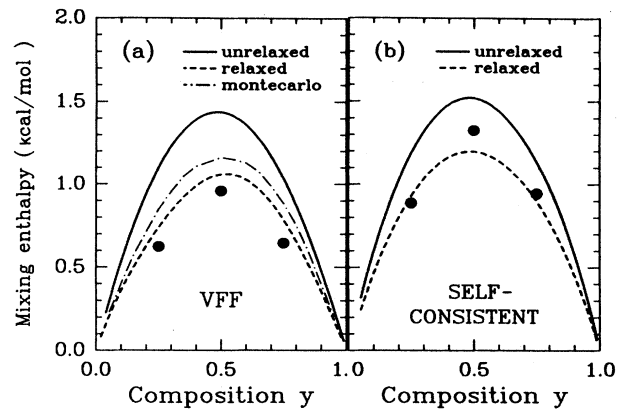


FIG. 10. Calculated enthalpy of mixing as a function of composition y , using (a) valence-force-field model; (b) self-consistent density-functional theory. Solid lines, model A ; dashed lines, model B ; dashed-dotted line, Monte Carlo results. The formation energies of the ordered structures are also shown (solid circles).

obtained using first-principles cluster energies. It is worth mentioning that the formation energies calculated using VFF are due to elastic deformations (elastic contribution). The difference between SC and VFF energies is due to the charge density redistribution (chemical contribution). The latter contribution can not be directly extracted from the figure, since the internal relaxation is not the same in both cases (larger in VFF).

Another important point to discuss is the spread of the NN distances. In model A , the NN distances are calculated using δ_{eq} of each tetrahedral configurations at the alloy lattice parameter $a(y)$. In Fig. 11(a) we show the calculated values, using this model, of the Ga-As (dashed lines) and Ga-Sb (dashed-dotted lines) NN distances as functions of composition. The important features to note are (i) in the unmixed configurations the Ga-As and Ga-Sb NN distances coincide with the Vegard's law variation

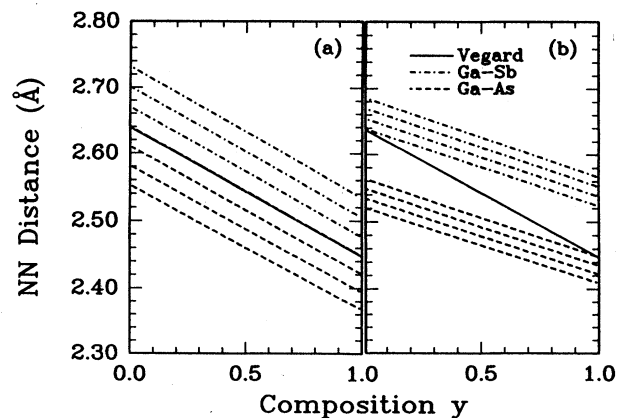


FIG. 11. Distribution of nearest-neighbor distances as a function of composition. (a) Model A ; (b) model B . Dashed lines, Ga-As; dashed-dotted lines, Ga-Sb; solid lines, Vegard's law.

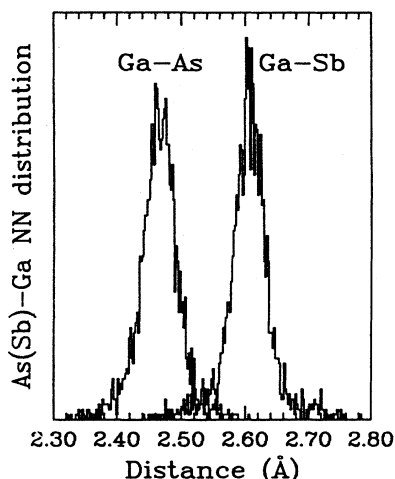


FIG. 12. Nearest-neighbor distances in $\text{GaAs}_{0.5}\text{Sb}_{0.5}$ calculated by Monte Carlo method.

and (ii) the large spread of the calculated distances. Both are in disagreement with experiment. Because of (i) the average bond lengths are closer to the Vegard's behavior than experimentally observed. To overcome this, the bond-bending contribution to the elastic energy has been completely neglected in previous VFF calculations.⁵⁰ In Fig. 11(b) we show the distances calculated using model *B*. For the sake of comparison, we show in Fig. 12 the distribution of the NNN distances obtained by the Monte Carlo simulation. It is clear that the distribution is in much better agreement with experiment. This leads to a more relaxed average NN distances (see Fig. 2), as expected.

VII. CONCLUSIONS

The thermodynamic properties of the $\text{GaAs}_y\text{Sb}_{1-y}$ pseudobinary alloy have been determined from a combination of *ab initio* total energy calculations and the modified quasicheical approximation. It has been verified that the cluster variation method gives the same results as QCA. The formation energies of five different ordered structures, corresponding to the various tetrahedral configurations, have been calculated within

the framework of the density-functional theory. The thermodynamic properties of the above alloys are calculated with fixed (model *A*) or relaxed (model *B*) NNN anion sublattice. The latter is simply accomplished by allowing the volume of each configuration to vary so that the average NNN distances reproduce the fully relaxed distances generated by the Monte Carlo simulation. We draw the following main conclusions.

(i) The formation energy of the ordered structures is found to be positive, leading to their disproportionation into the constituent binary compounds. This suggests that the recently observed¹⁴ ordering in $\text{GaAs}_{0.5}\text{Sb}_{0.5}$ epilayers is due to the presence of the substrate, and it is a moderate step toward complete segregation.

(ii) The strain energy is strongly reduced (by about 50%) by relaxing the NNN distances (model *B*) in the alloyed sublattice. The calculated miscibility gap using this model strictly reproduces the experimental gap, which lies approximately in the concentration range $0.2 < y < 0.8$, without any adjustable parameter as usually done in semiempirical models. The interaction parameter $\Omega = 4.75$ kcal/mole is also very close to the experimentally estimated value of 4.0–4.5 kcal/mole.

(iii) The calculated bimodal distribution of NN distances within model *B* is in better agreement with the EXAFS measurements than that obtained using model *A*.

(iv) The tendency to cluster is moderate and strongly dependent on the strain energy. The estimated clustering parameter is too low to explain the miscibility gap asymmetry, as suggested in Ref. 13.

ACKNOWLEDGMENTS

The authors are grateful to A. Baldereschi for providing his results before publication, and to R. Resta and A. Marbeuf for several illuminating discussions. One of us (A.Q.) has carried out this work with the support of the ICTP Program for Training and Research in Italian Laboratories, Trieste, Italy. This work has been partially supported by the Ministero della Pubblica Istruzione and the Gruppo Nazionale di Struttura della Materia del Consiglio Nazionale delle Ricerche of Italy (CISM-GNSM).

¹M. Podgorny and M. T. Czyżyk, Phys. Rev. B **36**, 2897 (1987).
²G. P. Srivastava, J. L. Martins, and A. Zunger, Phys. Rev. B **36**, 2902 (1987).
³J. W. D. Connolly and A. R. Williams, Phys. Rev. B **27**, 5169 (1983); A. A. Mbaye, L. G. Ferreira, and A. Zunger, Phys. Rev. Lett. **58**, 49 (1987).
⁴A. Qteish and R. Resta, Phys. Rev. B **37**, 6893 (1988).
⁵S. H. Wei, A. A. Mbaye, L. G. Ferreira, and A. Zunger, Phys. Rev. B **36**, 4183 (1987).
⁶M. T. Czyżyk, M. Podgorny, A. Balzarotti, P. Letardi, N. Motta, A. Kisiel, M. Zimnal-Starnawska, Z. Phys. B **62**, 133 (1986); P. Letardi, N. Motta, and A. Balzarotti, J. Phys. C **20**, 2853 (1987).

⁷P. N. Keating, Phys. Rev. **145**, 637 (1966); R. M. Martin, Phys. Rev. B **1**, 4005 (1970).
⁸R. Patrick, A. B. Chen, and A. Sher, Phys. Rev. B **36**, 6585 (1987).
⁹W. A. Harrison, *Electronic Structure and the Properties of Solids* (Freeman, San Francisco, 1980).
¹⁰A. Qteish, N. Motta, and A. Balzarotti, in Proceedings of the 19th International Conference on the Physics of Semiconductors, Warsaw (1988) (unpublished).
¹¹M. F. Grattton, and J. C. Woolley, J. Electrochem. Soc. **127**, 55 (1980).
¹²J. R. Pessetto and G. B. Stringfellow, J. Cryst. Growth **62**, 1 (1983).

- ¹³H. Mani, A. Jouillie, F. Karouta, and C. Schiller, *J. Appl. Phys.* **59**, 2728 (1985).
- ¹⁴H. R. Jen, M. J. Cherng, and G. B. Stringfellow, *Appl. Phys. Lett.* **48**, 1603 (1986).
- ¹⁵A. Ourmazd and J. C. Bean, *Phys. Rev. Lett.* **55**, 765 (1985).
- ¹⁶T. S. Kuan, T. K. Kuech, W. I. Wang, and E. L. Wilkie, *Phys. Rev. Lett.* **54**, 201 (1985).
- ¹⁷H. Nakayama and H. Fujita, in *GaAs and Related Compounds*, Inst. Phys. Conf. Ser. No. 79, edited by M. Fujimoto (Hilger, London, 1986).
- ¹⁸T. S. Kuan, W. I. Wang, and E. L. Wilkie, *Appl. Phys. Lett.* **51**, 51 (1987).
- ¹⁹M. A. Shahid, S. Mahajan, D. E. Loughlin and H. M. Cox, *Phys. Rev. Lett.* **58**, 2567 (1987).
- ²⁰A. Gomoyo, T. Suzuki, K. Kobayashi, S. Kawata, and I. Hino, *Appl. Phys. Lett.* **50**, 673 (1987).
- ²¹P. Hohemberg and W. Kohn, *Phys. Rev.* **136**, B864 (1964); W. Kohn and L. J. Sham, *ibid.* **140**, A133 (1965).
- ²²E. A. Guggenheim, *Mixture* (Oxford University Press, Oxford, 1952).
- ²³D. de Fontaine, in *Configurational Thermodynamics of Solid Solutions*, Vol. 34 of *Solid State Physics*, edited by H. Ehrenreich, F. Seitz and D. Turnbull (Academic, New York, 1979), p. 73.
- ²⁴D. M. Burley, in *Phase Transitions and Critical Phenomena*, edited by C. Domb and M. S. Green (Academic, London, 1972), p. 329.
- ²⁵M. Podgorny, M. T. Czyżyk, A. Balzarotti, P. Letardi, N. Motta, A. Kisiel, and M. Zimnal-Starnawska, *Solid State Commun.* **55**, 413 (1985).
- ²⁶R. Kikuchi, *J. Chem. Phys.* **60**, 1071 (1974).
- ²⁷C. H. Lupis, *Chemical Thermodynamics of Materials* (North-Holland, Amsterdam, 1983).
- ²⁸K. A. Jones, W. Porod, and D. K. Ferry, *J. Phys. Chem. Solids* **44**, 107 (1983).
- ²⁹*Theory of the Inhomogeneous Electron Gas*, edited by S. Lundqvist and N. H. March (Plenum, New York, 1983).
- ³⁰D. R. Hamann, M. Schlüter, and C. Chiang, *Phys. Rev. Lett.* **43**, 1494 (1979).
- ³¹D. M. Ceperley and B. J. Adler, *Phys. Rev. Lett.* **45**, 566 (1980).
- ³²J. Perdew and A. Zunger, *Phys. Rev. B* **23**, 5048 (1981).
- ³³G. Bachelet, D. R. Hamann, and M. Schlüter, *Phys. Rev. B* **26**, 4199 (1982).
- ³⁴A. Baldereschi, *Phys. Rev. B* **7**, 5212 (1973).
- ³⁵D. J. Chadi and M. L. Cohen, *Phys. Rev. B* **8**, 5747 (1973).
- ³⁶H. J. Monkhorst and J. D. Pack, *Phys. Rev. B* **13**, 5188 (1976).
- ³⁷A. Qteish and R. Resta, *Phys. Rev. B* **37**, 1308 (1988).
- ³⁸F. D. Murnaghan, *Proc. Nat. Acad. Sci. U.S.A.* **3**, 244 (1944).
- ³⁹P. Boguslawski and A. Baldereschi, in *Proceedings of the 19th International Conference on the Physics of Semiconductors*, Warsaw (1988) (unpublished).
- ⁴⁰S. Ciraci and I. P. Batra, *Phys. Rev. Lett.* **58**, 2114 (1987); *Phys. Rev. B* **36**, 1225 (1987).
- ⁴¹P. Boguslawski and A. Baldereschi, *Proceedings of the 17th International Conference on the Physics of Semiconductors* (Springer-Verlag, New York, 1985), p. 939.
- ⁴²G. P. Srivastava, J. L. Martins, and A. Zunger, *Phys. Rev. B* **31**, 2561 (1985).
- ⁴³G. Renaud, N. Motta, F. Lancon, and M. Belakhovsky, *Phys. Rev. B* **38**, 5944 (1988); *Solid State Commun.* **63**, 569 (1987).
- ⁴⁴N. Motta, A. Balzarotti, P. Letardi, A. Kisiel, M. T. Czyżyk, M. Zimnal-Starnawska, and M. Podgorny, *Solid State Commun.* **53**, 509 (1985).
- ⁴⁵N. Takenada, M. Inoue, J. Shirafyi, and J. Inuishi, *J. Phys. D* **11**, L91 (1978).
- ⁴⁶G. B. Stringfellow, *J. Cryst. Growth* **27**, 21 (1974); **58**, 194 (1982); M. B. Panish and M. Ilegems, *Prog. Solid State Chem.* **7**, 39 (1972).
- ⁴⁷A. Marbeuf, F. Karouta, H. Dexpert, P. Lagarde, and A. Jouille, *J. Phys. (Paris) Colloq.* **47**, C8-369 (1986).
- ⁴⁸A. Balzarotti, *Physica B* **146**, 150 (1987); M. Scheffler, *ibid.* **146**, 176 (1987).
- ⁴⁹T. M. Hayes and J. B. Boyce, in *Solid State Physics*, edited by H. Ehrenreich, F. Seitz, and D. Turnbull (Academic, New York, 1982), Vol. 3.
- ⁵⁰A. Balzarotti, A. Kisiel, N. Motta, M. Zimnal-Starnawska, M. T. Czyżyk, and M. Podgorny, *Phys. Rev. B* **30**, 2245 (1984); J. L. Martins and A. Zunger, *ibid.* **30**, 6217 (1984).